Mater. Res. Soc. Symp. Proc. Vol. 1322 © 2011 Materials Research Society
DOI: 10.1557/opl.2011.1293

Synthesis and Characterization of Rare Earth (Tb^{3+} and Yb^{3+}) Doped CdS/ZnS Core/Shell Nanocrystals for Enhanced Photovoltaic Efficiency

Sandip Das[1], and Krishna C. Mandal[1]
[1]Department of Electrical Engineering, University of South Carolina, Columbia, SC 29208, USA

ABSTRACT

CdS host nanocrystals with 4.2-5.5 nm in diameter have been synthesized from air stable precursors via a synthetic chemical route and doped with rare earth (RE) terbium (Tb^{3+}) and ytterbium (Yb^{3+}) ions. RE^{3+}-doped CdS cores were shelled by ZnS layers of different thicknesses. The resulting core/shell nanocrystals show a complete broadband absorption below 400-460 nm to the deep UV region depending on the size of the cores. RE^{3+}-doped CdS nanocrystals showed a red shift in the emission as observed under irradiation of 302 nm UV light and was confirmed by room temperature photoluminescence (PL) measurements. The nanocrystals were further characterized by x-ray diffraction (XRD), transmission electron microscopy (TEM), and energy dispersive x-ray (EDX) analysis. The results show that these RE^{3+}-doped nanocrystals can be used as solar spectral matching downconversion material to enhance photovoltaic efficiency of existing solar cells.

INTRODUCTION

Doped bulk and 2-D semiconductor materials have lead to the design and fabrication of the modern electronic and optoelectronic devices. However, for nanoscale functional optoelectronic materials and devices, doping of semiconductor nanocrystals is an interesting field of research. Recently, doped semiconductor nanocrystals have been reported to have tunable optoelectronic and magnetic properties [1, 2]. However, only a few materials have been investigated as dopants and exploration of new doping agents for various host nanocrystals offers an interesting scope of research in this area of study. Therefore, it is important to explore and investigate the properties of various semiconductor nanocrystals (NCs) doped with different dopants to fabricate novel functional nanomaterials and devices for future optoelectronic applications.

In this article we report rare earth (RE) doping of CdS nanocrystals by Tb^{3+} and Yb^{3+} and co-doped with these two RE ions. The RE^{3+}-doped CdS nanocrystals were characterized by Ultraviolet-Visible (UV-Vis) absorbance and room temperature photoluminescence (PL) measurements. Our results show that Tb^{3+} and Yb^{3+}-doped CdS nanocrytals show complete absorption below the band edge of the host CdS nanocrystals and a broadband emission in the visible region when excited below the band edge of the host CdS nanocrystals. This indicates that these RE-doped CdS nanocrystals can be used for optical downconversion, suitable for solar spectral matching to enhance solar cell efficiency. Doping of rare earth lanthanides to various host materials have been recently investigated for applications in Mid-IR Lasers [3, 4] and optical downconversion [5-9]. Although, many rare earth materials including Tb^{3+} and Yb^{3+} have been studied for downconversion applications [5-9], all of them were introduced either in phosphors, ceramics or in complex oxide host materials. In this article, for the first time, we report doping of CdS nanocrystals with rare earth Tb^{3+} and Yb^{3+}-ions and show its optical downconversion capability. Detailed synthetic procedure of RE^{3+}-doping of CdS nanocrystals

and characterization results of UV-Vis spectroscopy, room temperature PL, XRD, TEM, and EDX are presented in this article.

EXPERIMENTAL

Cadmium oxide (CdO, 99.99%) and zinc oxide (ZnO, 99.999%) were purchased from Strem Chemicals. Terbium acetate hydrate (99.9%) and ytterbium acetate hydrate (99.9%) were purchased from Alfa Aesar and Acros Organics respectively. Oleic acid (OA, 90%) was purchased from Alfa Aesar. 1-octadecene (ODE, tech. 90%) and oleylamine (OAm, tech. 70%) were purchased from Sigma-Aldrich. Sulfur Powder (99.5%) was obtained from Fisher Scientific. All precursors were used as received without any further purification. All steps of doped core/shell nanocrystal synthesis were carried out under high purity argon environment.

CdS cores were synthesized by a modified synthesis procedure reported by Peng et al, [10] using air stable oxide precursors dissolved in a noncoordinating solvent ODE, which produces high quality nearly monodisperse CdS nanocrystals of controllable size. In a typical synthesis, first the cadmium precursor solution was prepared by dissolving 51.2 mg of CdO (0.4 mmol) in a mixture of 3.8 ml OA and 15.8 ml of ODE at 290°C in a three-neck flask. Sulfur injection solution was prepared by dissolving 6.4 mg sulfur powder (0.2 mmol) in 5 ml ODE at 110°C. When completely dissolved, the as prepared sulfur solution was then cooled down to room temperature and quickly injected into the cadmium precursor solution held at 290°C to start the nucleation and growth of CdS nanocrystals. After injecting the sulfur solution, temperature of the reaction flask dropped to ~275°C and was maintained (±2°C) throughout the reaction time. In order to study the growth of the nanocrystals, multiple syntheses were carried out with different growth time and nanocrystals of varying sizes were obtained.

As grown CdS nanocrystals in the reaction mixture were extracted and purified by two repeated precipitation and decantation process. CdS cores in ODE phase was precipitated by adding adequate amount of acetone (~80 ml acetone for 20 ml reaction solution) followed by centrifugation at 17000×G. Precipitated nanocrystals were then dispersed in hexanes and further centrifuged to separate impurities and unreacted precursors. The cycle was repeated twice to get high quality nearly monodisperse CdS cores.

The rare earth doping was accomplished by modification of the reported method adopted for Mn^{2+}-doping of CdS nanocrystals [11]. We have chosen the respective RE-acetate salts for precursor preparation. Terbium and ytterbium precursor solutions were prepared by dissolving 10 µmol of the respective acetate salts in 4 ml of OAm at 150°C. When completely dissolved, the precursor solutions were cooled down to room temperature for further use. Sulfur precursor solution was prepared by mixing 1.6 mg (0.05 mmol) sulfur powder in 20 ml of ODE.

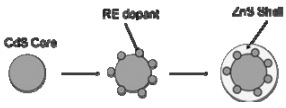

Figure 1. Schematic of surface doping mechanism

For ZnS shelling, a successive ion layer adsorption and reaction (SILAR) technique was adopted and the Zn precursor solution was prepared by dissolving ZnO in ODE and OA as reported by Mews et al [12]. Dopant growth and ZnS shelling was performed successively without any intermediate purification of the RE^{3+}-doped bare cores. We have adopted a surface doping scheme where the dopant atoms are localized at the core/shell interface as illustrated in figure 1.

In a typical RE dopant growth, the host CdS nanocrystals (~140 nmol) suspended in hexane was loaded into a three-neck flask and mixed with 15 ml of ODE and 5 ml of oleylamine (OAm). Hexanes and any other low vapor pressure solvents from the mixture were removed under vacuum and a homogeneous solution containing CdS cores in ODE and OAm was obtained. The solution temperature was increased to 265°C for dopant growth. 1 ml (equivalent to 2.5 µmol) of the as prepared respective dopant precursors (for Tb^{3+}-doping: 1 ml of Tb^{3+}-doping precursor; for Yb^{3+}-doping: 1 ml of Yb^{3+}-doping precursor; and for Tb^{3+}/ Yb^{3+} co-doping: mixture of 0.5 ml $Tb^{3+}$and 0.5 ml of Yb^{3+}-doping precursors in 1:1 ratio were used) was added drop by drop to the reaction flask and dopant growth was allowed for 30 minutes. Following, 1 ml (equivalent to 2.5 µmol) of the as prepared sulfur solution was added to the reaction flask and after 30 minutes, ZnS shelling was performed in a similar way by drop wise addition of Zn and sulfur precursors. After 3 monolayers ZnS shell growth, extraction and purification of the resulting doped core/shell nanocrystals were achieved.

RESULTS AND DISCUSSION

Optical characterization of the as-prepared, purified undoped and RE^{3+}-doped CdS nanocrystals were performed via UV-Vis absorbance (Perkin Elmer Lambda 750 spectrophotometer) and room temperature photoluminescence (PL) measurements (Horiba JOBIN-YVON Fluorolog 3 spectrofluorometer). Quartz cuvettes (Scientific Equipment of

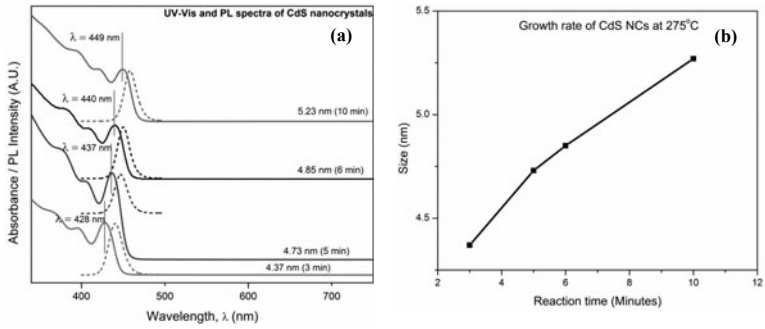

Figure 2. (a) UV-Vis and normalized PL spectra of undoped CdS nanocrystals, and (b) growth characteristics of CdS host nanocrystals with time.

Houston) with 190-2500 nm spectral range and 10 mm path length was used for both measurements. For PL measurement, slit width was kept constant at 2 nm in all occasions and the excitation wavelength was kept constant at 300 nm. Nanocrystals dispersed in hexanes were properly diluted to get absorbance value at the first excitonic peak below 0.1 for all samples in order to avoid nonlinear effects due to re-absorption.

Figure 2(a) shows the UV-Vis absorbance and room temperature PL spectra of purified undoped CdS host nanocrystals. The first excitonic absorption peak is red shifted with increased growth time indicating the formation of higher sized nanocrystals. Nanocrystal sizes were calculated by the empirical fitting function introduced by Peng et al [13] and the concentration

was calculated using lambart-beer's law. Calculated core sizes are plotted against time in figure 2(b), showing the growth characteristics of CdS cores at 275°C for our modified synthesis procedure.

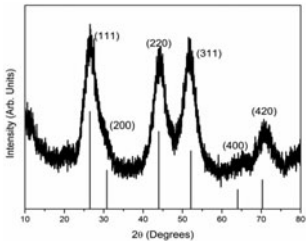

Figure 3. XRD pattern of CdS core nanocrystals.

The as grown nanocrystals were dried under argon, grinded to form a homogeneous powder and characterized by powder x-ray diffraction (XRD) using a Rigaku D/Max 2100 Powder X-ray Diffractometer (Cu Kα radiation) equipped with a diffracted beam graphite monochromator. The resulting diffraction pattern is shown in figure 3. The nanocrystals were found to be of Hawleyite (cubic) structure with side length of 5.818 nm. (111), (200), (220), (311), (400) and (420) peaks are identified and marked as shown. The best matching corresponding reference peaks are shown (in blue) as straight lines (JCPDS # 99-000-1489).

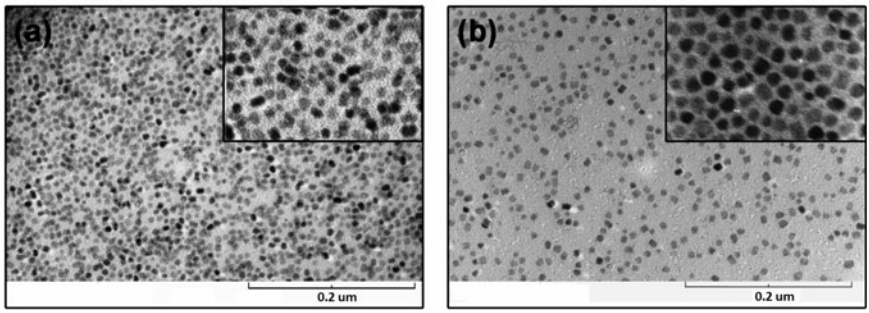

Figure 4. (a) TEM image of undoped CdS cores and (b) doped CdS/ZnS core/shell nanocrystals (Inset: same samples at 300K (cores) and 400K (core/shell) magnification).

TEM images were obtained by a Hitachi H-8000 TEM with an accelerating voltage of 200 KV (fig 4). The main images in figure 4 are taken at 120K magnification and inset images are taken at 300K (undoped CdS cores) and 400K (doped core/shell) magnification respectively. It is clearly seen that the synthesized NCs are very uniform and have narrow size distribution.

The compositional analysis of the undoped and doped CdS cores were performed by EDX using a FEI Quanta 200 ESEM and the results are presented in table I. It is observed that both undoped and doped nanocrystals are Cd rich and sulfur deficient. Compositional ratios were found consistent within a 0.3% tolerance at different places of the sample.

In figure 5, UV-Vis absorbance spectra of undoped and RE^{3+}-doped nanocrystals are shown. It is observed that all samples have a clear broadband absorption below 400-460 nm, depending on the band edge of the corresponding CdS host nanocrystals.

Table I. EDX data for undoped CdS and Tb^{3+}/Yb^{3+} co-doped CdS nanocrystals.

Sample	Elemental Composition (at%)			
	Cd	S	Tb	Yb
Undoped core	52.6	47.4	-	-
Co-doped core	49.6	49.1	0.6	0.7

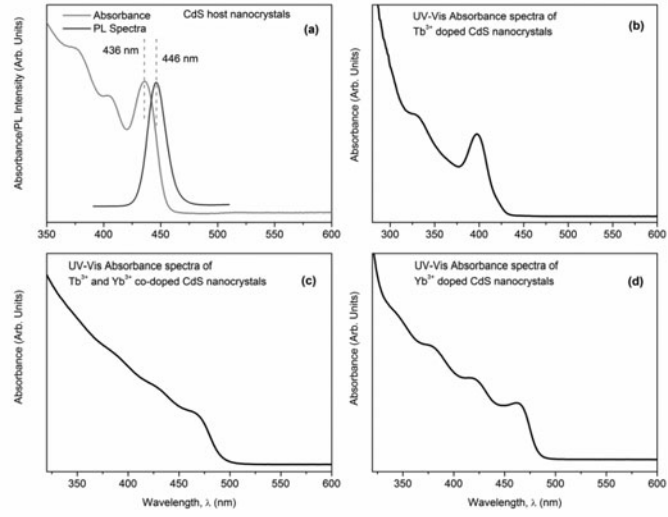

Figure 5. (a) UV-Vis and PL spectra of undoped CdS core; UV-Vis absorbance spectra of (b) Tb^{3+}-doped, (c) Yb^{3+}-doped and (d) Tb^{3+}/Yb^{3+} co-doped (1:1) CdS nanocrystals.

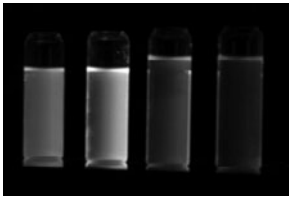

Figure 6. Optical photograph of room temperature emission from (left to right) undoped, Tb^{3+}-doped, Yb^{3+}-doped, Tb^{3+}/Yb^{3+} co-doped (1:1) CdS QDs.

Doped nanocrystals suspended in hexane were irradiated by a handheld UV lamp (UVM-57, 6W) irradiating 302 nm UV light. Figure 6 shows the room temperature optical photograph of undoped and doped nanocrystals (from left to right: undoped, Tb^{3+}-doped, Yb^{3+}-doped, Tb^{3+}/Yb^{3+} co-doped CdS QDs respectively) taken by a CCD digital camera under the UV irradiation. The red-shift of the emission is clearly visible from the optical photograph which was further confirmed by PL measurements.

The absorbance spectra and the normalized room temperature PL emission spectra for theTb^{3+}-doped and Tb^{3+}/Yb^{3+} co-doped CdS nanocrystals

are shown in the figure 7. It is observed that a broadband emission is emerged in the visible region after RE-doping of the CdS NCs. Tb^{3+}-doped CdS nanocrystals show a broadband emission in the visible region with the most pronounced peak at ~544 nm, which is attributed to the Tb^{3+}: $^5D_4 \rightarrow {}^7F_5$ transition. Also, a relatively less intense peak at ~670 nm can be observed which may be attributed to the emission due to surface defects.

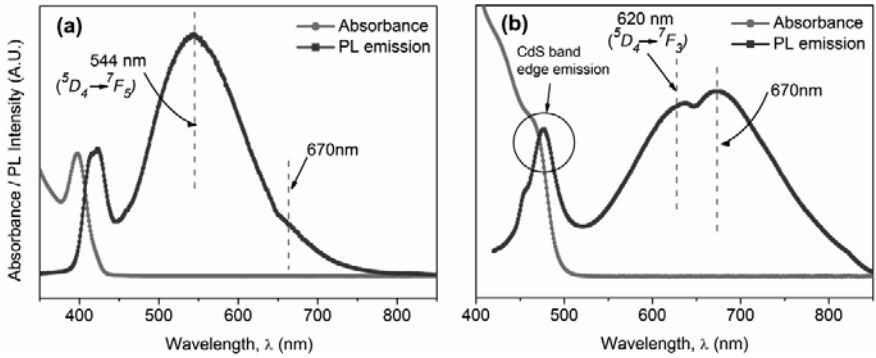

Figure 7. Absorbance and normalized PL emission spectra of (a) Tb^{3+}-doped and (b) Tb^{3+}/Yb^{3+} co-doped CdS nanocrystals.

We propose that the broadband nature of the emission spectra for doped nanocrystals is due to the superposition of $^5D_4 \rightarrow {}^7F_J$ (J=3,4,5,6) transitions of Tb^{3+} along with the mentioned defect induced emission. For Tb^{3+}/Yb^{3+} co-doped nanocrystals, the emission spectra is broader in the visible region and is more red shifted. However, the surface defect assisted emission (~670 nm) dominates in this system along with a comparable Tb^{3+}: $^5D_4 \rightarrow {}^7F_6$ transition peak at ~620 nm. Due to the scan window limitation (up to 1000 nm) of our measuring instrument (Horiba Jobin Yvon Fluorolog 3), we could not verify the possible Yb^{3+} *4f* transition in the infrared region above 1000 nm. The energy transition mechanism and relaxation dynamics for this co-doped system is currently under investigation. We believe that the defect assisted emission can be minimized and optical properties can further be improved by reducing the sulfur deficiency in the nanocrystals which will reduce bulk and surface defect densities. Optimization of the optical properties of these RE-doped NCs are presently under investigation and will be reported in future.

CONCLUSIONS

We have successfully doped CdS host nanocrystals with rare earth (RE) ions, namely terbium (Tb^{3+}) and ytterbium (Yb^{3+}) by a simple synthetic chemical route. The nanocrystals were also co-doped by these RE ions. We have demonstrated optical down-conversion of high energy UV photons using these novel materials. Host CdS nanocrystals were of cubic structure and were found to be nearly monodisperse as confirmed by sharp absorption peak and TEM images. Optical characterization results indicate a complete absorption when excited below the band edge of host CdS cores and a broad band emission in the visible region is observed for the RE^{3+}-doped

nanocrystals. This result suggests that these RE-doped nanocrystals can be used as a down-converting material for harvesting higher energy UV photons which can lead to an enhanced photovoltaic efficiency. Optimization of the optical properties with doping concentration and dopant locale in the core/shell structure and detailed study of energy transfer mechanism are presently under investigation.

ACKNOWLEDGEMENTS

We acknowledge financial support by DARPA (grant # N66001-10-1-4031) for this investigation. We are thankful to Dr. MVS Chandrashekhar and Ramesh M. Krishna for helping with UV-Vis/PL, and EDX measurements.

REFERENCES

1. Heesun Yang, and Paul H. Holloway, *Appl. Phys Lett.*, **82** (2003) 1965.
2. Ruosheng Zeng, Michael Rutherford, Renguo Xie, Bingsuo Zou, andXiaogang Peng, *Chem. Mater.*, **22** (2010) 2107.
3. Krishna C. Mandal, Sung H. Kang, Michael Choi, and R. David Rauh, *Int. J. High Speed Electronics and Sys.*, **18** (2008) 735.
4. Katja Rademaker, William F. Krupke, Ralph H. Page, Stephen A. Payne, Klaus Petermann, Guenter Huber, Alexander P. Yelisseyev, Ludmila I. Isaenko, Utpal N. Roy, Arnold Burger, Krishna C. Mandal, and Karel Nitsch, *J. Opt. Soc. Am. B*, **21** (2004) 2117.
5. X. Y. Huang, D.C. Yu, and Q.Y. Zhang, *J. Appl. Phys.*, **106** (2009) 113521.
6. Song Ye, Bin Zhu, Jingxin Chen, Jin Luo, and Jian Rong Qiu, *Appl. Phys. Lett.*, **92** (2008) 141112.
7. Yuhua Wang, Lechun Xie, and Huijuan Zhang, *J. Appl. Phys.*, **105** (2009) 023528.
8. Te-Ju Lee, Li-Yang Luo, Eric Wei-Guang Diau, and Teng-Ming Chen, *Appl. Phys. Lett.*, **89** (2006) 131121.
9. Qiuhong Zhang, Jing Wang, Gongguo Zhang, and Qiang Su, *J. Mater. Chem.*, **19** (2009) 7088.
10. W. William Yu, and Xiaogang Peng, *Angew. Chem. Int. Ed.*, **41** (2002) 2368
11. Yongan Yang, Ou Chen, Alexander Angerhofer, and Charles Cao, *J. Am. Chem. Soc.*, **130** (2008) 15649.
12. Renguo Xie, Ute Kolb, Jixue Li, Thomas Basché, and Alf Mews, *J. Am. Chem. Soc.*, **127** (2005) 7480.
13. W. William Yu, Lianhua Qu, Wenzhuo Guo, and Xiaogang Peng, *Chem. Mater.*, **15** (2003), 2854.